

A SIZE-DEPENDENT FINITE-ELEMENT MODEL FOR A MICRO/NANOSCALE TIMOSHENKO BEAM

Long Zhang,¹ Binglei Wang,^{1,2,*} Binbin Liang,¹ Shenjie Zhou,³ & Yiguo Xue¹

¹School of Civil Engineering, Shandong University, Jinan, 250061, China

²State Key Laboratory for Strength and Vibration of Mechanical Structures, School of Aerospace, Xi'an Jiaotong University, Xi'an 710049, China

³School of Mechanical Engineering, Shandong University, Jinan, 250061, China

*Address all correspondence to Binglei Wang, E-mail: bwang@sdu.edu.cn

A size-dependent finite-element model for a micro/nanoscale Timoshenko beam is developed based on the strain gradient elasticity theory. The newly developed element contains three material length scale parameters that capture the size effect. This element is a new, comprehensive Timoshenko beam element that can reduce to the modified couple stress Timoshenko beam element or the classical Timoshenko beam element if two (l_0 and l_1) or three (l_0 , l_1 , and l_2) material length scale parameters are set to zero. The element satisfies C_0 continuity and C_1 weak continuity and has two nodes, with four degrees of freedom at each node considering only bending deformation. The deflection and cross-sectional rotation of the element are interpolated independently. The finite-element formulations and the stiffness and mass matrices are derived using the corresponding weak-form equations. To verify the reliability and accuracy of the proposed element, the problems of convergence and shear locking are studied. Using the newly developed element, the static bending and free vibration problems of the clamped and simply supported Timoshenko microbeam are investigated. The results for a simply supported Timoshenko microbeam predicted by the new element model agree well with results from the literature. Moreover, the results illustrate that the size effect on the Timoshenko microbeam can be effectively predicted by using the proposed element.

KEY WORDS: *microscale, Timoshenko beam element, strain gradient elasticity theory, size effect*

1. INTRODUCTION

Rapid progress in device miniaturization has led to the quick rise of micro/nanobeam-like structures in micro/nano-electromechanical systems (MEMS/NEMS) or atomic force microscopes (AFMs) because of their superior mechanical, chemical, and electronic properties. For this reason, accurate modeling and analysis of the static and dynamic behaviors of micro/nanobeams are crucial to research. The characteristic size of these beams is comparable to the material microstructure (e.g., the grain size or atomic lattice spacing), which leads to distinct mechanical behaviors with respect to their macroscopic counterparts. Numerous experiments have observed size-dependent behaviors in metals (Poole et al., 1996), brittle materials (Vardoulakis et al., 1998), polymers (Lam and Chong, 1999; Lam et al., 2003; McFarland and Colton, 2005), and polysilicon (Chasiotis and Knauss, 2003; Sadeghian et al., 2011). These behaviors cannot be explained using classical continuum theory, which has no length-scale parameters (MLSPs). Hence, the size effect must be taken into account in theoretical and experimental studies.

Recently, size-dependent continuum theories have received increasing attention in the modeling of micro/nano-structures and devices. These include nonlocal continuum theory (Eringen, 1983), surface energy theory (Gurtin and Murdoch, 1975), couple stress theory (Yang et al., 2002), and strain gradient elasticity theory (Lam et al., 2003).

When applying nonlocal theory, a paradoxical conclusion arises: the small length scale effect vanishes in the bending deflection for the Euler-Bernoulli cantilever nanobeam under a transverse point load. Moreover, this theory predicts a “softening effect”, which is inconsistent with the “stiffening effect” observed in experiments (Lam et al., 2003). For surface energy theory, it is considered that surface properties cannot be overlooked in the study of nanostructures and nanomaterials because of the large value of surface–volume ratios at that scale (Assadi, 2013). Although this theory is applied to size-dependent behaviors, it must be admitted that the mechanical properties are relative not only to the surface part but also to the internal part because the characteristic length is in the bulk, such as grain size or atomic lattice spacing.

The couple stress theory is a nonclassical continuum theory in which higher-order stresses, known as couple stresses, exist (Koiter, 1964). Yang et al. (2002) proposed a modified theory involving only one additional MLSP. Since then, numerical approaches have been developed to study the size effect of the linear and nonlinear Bernoulli–Euler beam (Fathalilou et al., 2014; Park and Gao, 2006; Xia et al., 2010), the linear and nonlinear Timoshenko beam (Asghari et al., 2010b; Ma et al., 2008), the linear functionally graded Euler-Bernoulli beam (Asghari et al., 2010a), the Timoshenko beam (Asghari et al., 2011), the Kirchhoff plate (Tsiatas, 2009), and the pull-in phenomena in MEMS (Yin et al., 2011).

Of the most popular size-dependent continuum models, the strain gradient elasticity theory (Lam et al., 2003), a modification of Mindlin’s linear elasticity theory for microstructures (Mindlin, 1964), is widely used. It introduces three MLSPs to characterize the dilatation gradient tensor, the deviatoric stretch gradient tensor, and the symmetric rotation gradient tensor. Also, the higher-order stress tensor work-conjugate to the new higher-order deformation metrics and the corresponding constitutive relations are defined. As our previous papers have pointed out (Wang et al., 2010), the strain gradient elasticity theory can reduce to the modified couple stress theory (Yang et al., 2002) if two of the three MLSPs are set to zero. This indicates that it is a more general theory than the modified couple stress theory (Yang et al., 2002). The strain gradient elasticity theory has been applied to study the linear (Kong et al., 2009) and nonlinear (Zhao et al., 2012) Euler beam, the linear (Wang et al., 2010) and nonlinear (Asghari et al., 2010b) Timoshenko beam, and the Reddy-Levinson beam (Wang et al., 2014). It has also been employed to investigate size-dependent pull-in phenomena in MEMS (Wang et al., 2011a,b, 2012).

Higher-order continuum theories are more complicated than conventional elasticity theory. Higher-order terms (e.g., strain gradient) are incorporated in the governing equations and boundary conditions, leading to difficulties in problem solutions. In our experience, only a few cases with simple geometric shapes and boundary conditions can be achieved with exact analytical solutions. Moreover, for micro/nanobeams the presence of complex forces such as Casimir, Van Der Waals, and capillary forces may introduce unexpected nonlinearities.

Naturally, approaches other than analytical ones are required to deal with the problems occurring in micro/nanobeams. The finite-element method (FEM) is one of the most popular numerical alternatives and has been used to investigate the mechanical behavior of micro/nanoscale structures based not only on classical continuum theory but also on the size-dependent theories mentioned previously.

Phadikar and Pradhan (2010) presented a finite-element formulation for nonlocal elastic nanobeams and nanoplates based on nonlocal elasticity theory. Pradhan (2012) proposed a finite-element formulation for nonlocal elastic Bernoulli-Euler beam and Timoshenko beam theories. Based on the modified couple stress theory, Kahrobaiyan et al. (2014) developed a size-dependent Timoshenko beam element model to predict the size dependence observed in microbeams. Zhang et al. (2013) proposed a novel Mindlin plate element based on the framework of modified couple stress theory for analyzing the static bending, free vibration, and buckling behaviors of size-dependent Mindlin microplates. The finite-element method is also used to develop the size-dependent Euler–Bernoulli beam element based on the strain gradient theory (Kahrobaiyan et al., 2013). Also based on the strain gradient elasticity theory, the size-dependent nonclassical Timoshenko beam element model (Zhang et al., 2014) was proposed for predicting the mechanical behaviors of microbeams where six-degree-of-freedom (6-DOF) nodes are introduced.

Our previous work established the theoretical size-dependent Timoshenko beam model based on the strain gradient theory. In the present study, the corresponding finite-element approach is adopted to predict the mechanical behaviors of micro/nanoscale beams, which is the main gap we try to bridge.

The rest of the paper is organized as follows. In Section 2, the size-dependent Timoshenko beam model, based on the strain gradient elasticity theory, is reviewed. The finite-element formulations as well as the weak-form formulations

of the model are presented in Section 3, which introduces a two-node element where each node has 4 DOF. Numerical examples and discussions are given in Section 4. Finally, conclusions are summarized in Section 5.

2. THEORETICAL FORMULATIONS

2.1 Size-Dependent Timoshenko Beam Model

The strain gradient theory proposed by Lam et al. (2003) introduces three independent material length scale parameters for isotropic linear elastic materials in addition to two classical material constants. Then the strain energy U in a deformed isotropic linear elastic material occupying region Ω is written as

$$U = \frac{1}{2} \int_{\Omega} (\sigma_{ij} \varepsilon_{ij} + p_i \gamma_i + \tau_{ijk}^{(1)} \eta_{ijk}^{(1)} + m_{ij}^s \chi_{ij}^s) d\Omega \tag{1}$$

The deformed measures—strain tensor ε_{ij} , dilatation gradient tensor γ_i , deviatoric stretch gradient $\eta_{ijk}^{(1)}$, and symmetric rotation gradient χ_{ij}^s —are defined as

$$\varepsilon_{ij} = \frac{1}{2} (u_{i,j} + u_{j,i}) \tag{2}$$

$$\gamma_i = \varepsilon_{mm,i} \tag{3}$$

$$\eta_{ijk}^{(1)} = \eta_{ijk}^s - \frac{1}{5} (\delta_{ij} \eta_{mmk}^s + \delta_{jk} \eta_{mmi}^s + \delta_{ki} \eta_{mmj}^s) \tag{4}$$

$$\chi_{ij}^s = \frac{1}{2} (e_{ipq} \varepsilon_{qj,p} + e_{j pq} \varepsilon_{qi,p}) \tag{5}$$

where u_i is the displacement vector, ε_{mm} is the dilatation strain, δ_{ij} and e_{ijk} are the Kronecker symbol and the alternate symbol, respectively, and η_{ijk}^s is the symmetric part of the second-order displacement gradient tensor, given by

$$\eta_{ijk}^s = \frac{1}{3} (u_{i,jk} + u_{j,ki} + u_{k,ij}) \tag{6}$$

It should be noted that the index notation is always used with repeated indices denoting summation from 1 to 3.

The corresponding stress measures are respectively given by the following constitutive relations:

$$\sigma_{ij} = k \delta_{ij} \varepsilon_{mm} + 2\mu \varepsilon'_{ij} \tag{7}$$

$$p_i = 2\mu l_0^2 \gamma_i \tag{8}$$

$$\tau_{ijk}^{(1)} = 2\mu l_1^2 \eta_{ijk}^{(1)} \tag{9}$$

$$m_{ij}^s = 2\mu l_2^2 \chi_{ij}^s \tag{10}$$

where ε'_{ij} is the deviatoric strain, defined as

$$\varepsilon'_{ij} = \varepsilon_{ij} - \frac{1}{3} \varepsilon_{mm} \delta_{ij} \tag{11}$$

In the previous equations, l_0 , l_1 , and l_2 are the additional independent material length scale parameters associated with the dilatation gradients, deviatoric stretch gradients, and symmetric rotation gradients, respectively. The parameters k and μ in the constitutive equation of classical stress σ_{ij} are bulk and shear modulus, respectively. They can be written in terms of Young's modulus E and the Poisson ratio ν as

$$k = \frac{E}{3(1-2\nu)}, \quad \mu = \frac{E}{2(1+\nu)} \tag{12}$$

As shown in Fig. 1, a straight beam subjected to a static lateral load $q(x)$ distributed along the longitudinal axis x of the beam is considered, where the loading plane coincides with the xz -plane and the cross-section parallels the yz -plane. The displacement fields, based on Timoshenko beam theory, can be described as (Dym and Shames, 1973)

$$u_1(x, y, z, t) = -z\psi(x, t), \quad u_2(x, y, z, t) = 0, \quad u_3(x, y, z, t) = w(x, t) \quad (13)$$

where t is time, and $\psi(x, t)$ is the rotation of line elements along the centerline due to bending only. Here we assume that the shear strain is the same at all points over a given cross-section of the beam.

By substituting Eq. (13) into Eq. (2), the nonzero components of the strain tensor can be obtained:

$$\varepsilon_{11} = -z \frac{\partial \psi}{\partial x}, \quad \varepsilon_{13} = \varepsilon_{31} = \frac{1}{2} \left(\frac{\partial w}{\partial x} - \psi \right) \quad (14)$$

Using Eqs. (3) and (14), the nonzero components of the dilatation gradient tensor γ_i can be obtained:

$$\gamma_1 = -z \frac{\partial^2 \psi}{\partial x^2}, \quad \gamma_3 = -\frac{\partial \psi}{\partial x} \quad (15)$$

Inserting Eqs. (14) into Eq. (5) yields the nonzero components of the symmetric rotation gradient χ_{ij}^s :

$$\chi_{12}^s = \chi_{21}^s = -\frac{1}{4} \left(\frac{\partial^2 w}{\partial x^2} + \frac{\partial \psi}{\partial x} \right) \quad (16)$$

From Eqs. (4), (6), and (13), the nonzero components of the deviatoric stretch gradient $\eta_{ijk}^{(1)}$, we have

$$\begin{aligned} \eta_{111}^{(1)} &= -\frac{2}{5} z \frac{\partial^2 \psi}{\partial x^2}, & \eta_{333}^{(1)} &= -\frac{1}{5} \left(\frac{\partial^2 w}{\partial x^2} - 2 \frac{\partial \psi}{\partial x} \right) \\ \eta_{113}^{(1)} &= \eta_{311}^{(1)} = \eta_{131}^{(1)} = \frac{4}{15} \left(\frac{\partial^2 w}{\partial x^2} - 2 \frac{\partial \psi}{\partial x} \right), & \eta_{221}^{(1)} &= \eta_{122}^{(1)} = \eta_{212}^{(1)} = \frac{1}{5} z \frac{\partial^2 \psi}{\partial x^2} \\ \eta_{223}^{(1)} &= \eta_{322}^{(1)} = \eta_{232}^{(1)} = -\frac{1}{15} \left(\frac{\partial^2 w}{\partial x^2} - 2 \frac{\partial \psi}{\partial x} \right), & \eta_{331}^{(1)} &= \eta_{133}^{(1)} = \eta_{313}^{(1)} = \frac{1}{5} z \frac{\partial^2 \psi}{\partial x^2} \end{aligned} \quad (17)$$

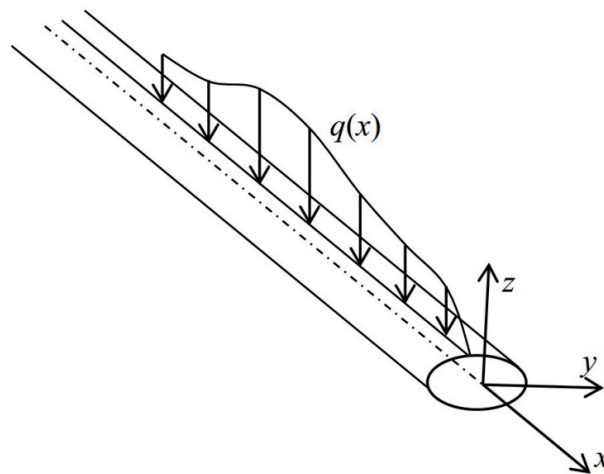


FIG. 1: Geometry and loading of the Timoshenko beam

The nonzero stresses σ_{ij} can be obtained using Eqs. (14), (11), and (7):

$$\sigma_{11} = -z \left(k + \frac{4}{3}\mu \right) \frac{\partial \psi}{\partial x}, \quad \sigma_{22} = \sigma_{33} = -z \left(k - \frac{2}{3}\mu \right) \frac{\partial \psi}{\partial x}, \quad \sigma_{13} = \sigma_{31} = \mu \left(\frac{\partial w}{\partial x} - \psi \right) \quad (18)$$

It is worth noting that the σ_{13} and σ_{31} variations depend only on x . To take the nonuniformity of the shear strain into account over the beam cross-section, a correction factor k_s , which depends on the shape of the cross-section, is introduced to the stress components σ_{13} and σ_{31} as follows:

$$\sigma_{13} = \sigma_{31} = k_s \mu \left(\frac{\partial w}{\partial x} - \psi \right) \quad (19)$$

Substituting Eq. (15) into Eq. (8) yields

$$p_1 = -2\mu l_0^2 z \frac{\partial^2 \psi}{\partial x^2}, \quad p_3 = -2\mu l_0^2 \frac{\partial \psi}{\partial x} \quad (20)$$

From Eqs. (16) and (10), it follows that

$$m_{12}^s = m_{21}^s = -\frac{1}{2} \mu l_2^2 \left(\frac{\partial^2 w}{\partial x^2} + \frac{\partial \psi}{\partial x} \right) \quad (21)$$

From Eqs. (9) and (17), the nonzero components of the higher-order stresses $\tau_{ijk}^{(1)}$ are

$$\begin{aligned} \tau_{111}^{(1)} &= -\frac{4}{5} z \mu l_1^2 \frac{\partial^2 \psi}{\partial x^2}, & \tau_{333}^{(1)} &= -\frac{2}{5} \mu l_1^2 \left(\frac{\partial^2 w}{\partial x^2} - 2 \frac{\partial \psi}{\partial x} \right) \\ \tau_{113}^{(1)} &= \tau_{311}^{(1)} = \tau_{131}^{(1)} = \frac{8}{15} \mu l_1^2 \left(\frac{\partial^2 w}{\partial x^2} - 2 \frac{\partial \psi}{\partial x} \right), & \tau_{221}^{(1)} &= \tau_{122}^{(1)} = \tau_{212}^{(1)} = \frac{2}{5} z \mu l_1^2 \frac{\partial^2 \psi}{\partial x^2} \\ \tau_{223}^{(1)} &= \tau_{322}^{(1)} = \tau_{232}^{(1)} = -\frac{2}{15} \mu l_1^2 \left(\frac{\partial^2 w}{\partial x^2} - 2 \frac{\partial \psi}{\partial x} \right), & \tau_{331}^{(1)} &= \tau_{133}^{(1)} = \tau_{313}^{(1)} = \frac{2}{5} z \mu l_1^2 \frac{\partial^2 \psi}{\partial x^2} \end{aligned} \quad (22)$$

According to Hamilton's principle, the actual motion minimizes the difference between the kinetic energy and the total potential energy for a system with prescribed configurations at t_1 and t_2 . That is,

$$\delta \int_{t_1}^{t_2} [T - (U - W)] dt = 0 \quad (23)$$

The variation in strain energy U can be expressed as

$$\begin{aligned} \delta U &= \delta \frac{1}{2} \int_{\Omega} \left(\sigma_{ij} \varepsilon_{ij} + p_i \gamma_i + \tau_{ijk}^{(1)} \eta_{ijk}^{(1)} + m_{ij}^s \chi_{ij}^s \right) dV = \int_{\Omega} \left(\sigma_{ij} \delta \varepsilon_{ij} + p_i \delta \gamma_i + \tau_{ijk}^{(1)} \delta \eta_{ijk}^{(1)} + m_{ij}^s \delta \chi_{ij}^s \right) dV \\ &= \int_0^L \left[(k_3 + k_4) w^{IV} + (k_3 - 2k_4) \psi''' + k_5 (-w'' + \psi) \right] \delta w dx + \int_0^L \left[k_1 \psi^{IV} - (k_3 - 2k_4) w''' \right. \\ &\quad \left. - (k_2 + k_3 + 4k_4) \psi'' + k_5 (-w' + \psi) \right] \delta \psi dx + [-(k_3 + k_4) w''' + (-k_3 + 2k_4) \psi'' + k_5 (w' - \psi)] \delta w \Big|_0^L \\ &\quad + [(k_3 + k_4) w'' + (k_3 - 2k_4) \psi'] \delta w \Big|_0^L + [-k_1 \psi''' + (k_3 - 2k_4) w'' + (k_2 + k_3 + 4k_4) \psi'] \delta \psi \Big|_0^L + k_1 \psi'' \delta \psi \Big|_0^L \end{aligned} \quad (24)$$

where

$$k_1 = I \left(2\mu l_0^2 + \frac{4}{5} \mu l_1^2 \right), \quad k_2 = I \left(k + \frac{4}{3} \mu \right) + 2\mu A l_0^2, \quad k_3 = \frac{1}{4} \mu A l_2^2, \quad k_4 = \frac{8}{15} \mu A l_1^2, \quad k_5 = k_s \mu A \quad (25)$$

The variation in the kinetic energy of the beam can be expressed as

$$\delta T = \delta \int_V \frac{1}{2} \rho \left[\left(\frac{\partial u_1}{\partial t} \right)^2 + \left(\frac{\partial u_2}{\partial t} \right)^2 + \left(\frac{\partial u_3}{\partial t} \right)^2 \right] dV = \int_0^L \left(m_0 \dot{w} \delta \dot{w} + m_2 \dot{\psi} \delta \dot{\psi} \right) dx \quad (26)$$

where

$$m_0 = \rho A, \quad m_2 = \rho I, \quad I = \int_A z^2 dA \quad (27)$$

The first variation of the work done by the external force, $q(x, y)$, takes the form

$$\delta W = \int_0^L q(x) \delta w dx + V \delta w|_0^L + M \delta \psi|_0^L + M_h \delta \psi'|_0^L \quad (28)$$

Because of the fundamental lemma of the calculus of variation with the arbitrariness of δw and $\delta \psi$ for the given $x \in [0, L]$ and $t \in [t_1, t_2]$, the governing equations for the beam in bending are given by

$$\begin{aligned} m_0 \ddot{w} - q + (k_3 + k_4) w^{IV} + (k_3 - 2k_4) \psi''' + k_5 (-w'' + \psi') &= 0 \\ m_2 \ddot{\psi} + k_1 \psi^{IV} - (k_3 - 2k_4) w''' - (k_2 + k_3 + 4k_4) \psi'' + k_5 (-w' + \psi) &= 0 \end{aligned} \quad (29)$$

and the boundary conditions can be written as

$$\left. \begin{aligned} (k_3 + k_4) w''' + (k_3 - 2k_4) \psi'' - k_5 (w' - \psi) &= -\bar{V} \quad \text{or} \quad w = \bar{w} \\ (k_3 + k_4) w'' + (k_3 - 2k_4) \psi' &= 0 \quad \text{or} \quad w' = \bar{w}' \\ -k_1 \psi''' + (k_3 - 2k_4) w'' + (k_2 + k_3 + 4k_4) \psi' &= \bar{M} \quad \text{or} \quad \psi = \bar{\psi} \\ k_1 \psi'' = \bar{M}_h \quad \text{or} \quad \psi' = \bar{\psi}' \end{aligned} \right\} \quad \text{at } x = 0 \quad \text{and} \quad x = L \quad (30)$$

The boundary conditions are determined by specifying the kinematic boundary conditions or by satisfying the natural boundary conditions (Dym and Shames, 1973).

2.2 Weak-Form Equations for the Timoshenko Beam

For the static analysis of Timoshenko beams, a weak form can be briefly expressed as

$$\begin{aligned} \int_0^L \left[(k_3 + k_4) w'' \delta w'' + (k_3 - 2k_4) \psi' \delta w'' - k_5 (-w' + \psi) \delta w' + k_1 \psi'' \delta \psi'' + (k_3 - 2k_4) w'' \delta \psi' \right. \\ \left. + (k_2 + k_3 + 4k_4) \psi' \delta \psi' + k_5 (-w' + \psi) \delta \psi \right] dx = \int_0^L q(x) \delta w dx + (N_w^{(0)} \delta w + N_w^{(1)} \delta w' \\ + N_\psi^{(0)} \delta \psi + N_\psi^{(1)} \delta \psi') \Big|_0^L \end{aligned} \quad (31)$$

in which

$$\begin{aligned} N_w^{(0)} &= (k_3 + k_4) w''' + (k_3 - 2k_4) \psi'' - k_5 (w' - \psi) \\ N_w^{(1)} &= (k_3 + k_4) w'' + (k_3 - 2k_4) \psi' \\ N_\psi^{(0)} &= -k_1 \psi''' + (k_3 - 2k_4) w'' + (k_2 + k_3 + 4k_4) \psi' \\ N_\psi^{(1)} &= k_1 \psi'' \end{aligned} \quad (32)$$

For the free vibration analysis of Timoshenko beams, a weak form can be briefly expressed as

$$\begin{aligned} \int_0^L \left[(k_3 + k_4) w'' \delta w'' + (k_3 - 2k_4) \psi' \delta w'' - k_5 (-w' + \psi) \delta w' + k_1 \psi'' \delta \psi'' + (k_3 - 2k_4) w'' \delta \psi' \right. \\ \left. + (k_2 + k_3 + 4k_4) \psi' \delta \psi' + k_5 (-w' + \psi) \delta \psi \right] dx = - \int_0^L \left(m_0 \frac{\partial^2 w}{\partial t^2} \delta w + m_2 \frac{\partial^2 \psi}{\partial t^2} \delta \psi \right) dx \\ + \left(N_w^{(0)} \delta w + N_w^{(1)} \delta w' + N_\psi^{(0)} \delta \psi + N_\psi^{(1)} \delta \psi' \right) \Big|_0^L \end{aligned} \quad (33)$$

3. FINITE-ELEMENT FORMULATIONS

In this section, the stiffness and mass matrices of a Timoshenko microbeam element are derived. The appropriate shape functions are given by the Hermite polynomial. The weak-form equations for Timoshenko microbeams are discretized to finite elements using the finite-element method. From Eqs. (31) and (33), it can be seen that the weak-form equations contain the second-order derivative of transverse deflection w and rotation ψ . However, because weak-form equations based on classical Timoshenko beam theory contain only the first derivative of generalized displacements, the generalized displacement functions need to satisfy C_1 continuity to guarantee the weak-form equations' integrability. In this paper, a two-node Timoshenko beam element with 4 DOF at each node is proposed that satisfies both C_0 continuity and C_1 weak continuity conditions and includes three material length scale parameters to capture the microstructure size effect.

The deflection and the cross-sectional rotation of the element are interpolated independently. According to FEM, the element's displacement w and rotation ψ are related to the corresponding nodal displacement vector as

$$w = \mathbf{N}_w \mathbf{a}_w, \quad \psi = \mathbf{N}_\psi \mathbf{a}_\psi \quad (34)$$

where the nodal displacement vector \mathbf{a} for the new beam element can be represented as

$$\mathbf{a}_w = [w_1 \quad w'_1 \quad w_2 \quad w'_2]^T, \quad \mathbf{a}_\psi = [\psi_1 \quad \psi'_1 \quad \psi_2 \quad \psi'_2]^T \quad (35)$$

\mathbf{N}_w and \mathbf{N}_ψ represent the shape function matrices for displacement and rotation, respectively:

$$\mathbf{N}_w = [N_1^w \quad N_2^w \quad N_3^w \quad N_4^w], \quad \mathbf{N}_\psi = \mathbf{N}_w \quad (36)$$

The appropriate shape functions are given by the first-order Hermite polynomial, which is given as

$$\begin{aligned} N_1^w &= 1 - 3\left(\frac{x}{L}\right)^2 + 2\left(\frac{x}{L}\right)^3, & N_2^w &= \left[\frac{x}{L} - 2\left(\frac{x}{L}\right)^2 + \left(\frac{x}{L}\right)^3\right]L \\ N_3^w &= 3\left(\frac{x}{L}\right)^2 - 2\left(\frac{x}{L}\right)^3, & N_4^w &= \left[-\left(\frac{x}{L}\right)^2 + \left(\frac{x}{L}\right)^3\right]L \end{aligned} \quad (37)$$

By substituting Eq. (34) into the weak-form equations [Eqs. (31) and (33)], respectively, the finite-element formulations for the static bending and free vibration problems of Timoshenko microbeams can be obtained, along with the stiffness and mass matrices of the new element. Because the forms \mathbf{K}^e and \mathbf{M}^e are tedious and complicated, they are given in the Appendix.

For the static model, the formulation of the Timoshenko beam element can be written as

$$\mathbf{Kd} = \mathbf{F} \quad (38)$$

For the free vibration problem, it can be written as

$$(\mathbf{K} - \omega^2 \mathbf{M})\mathbf{d} = \mathbf{0} \quad (39)$$

in which \mathbf{K} , \mathbf{F} , and \mathbf{M} are the global stiffness matrix, the global force vector, and the global mass matrix, respectively, and ω is the natural frequency. By assembling each corresponding element matrix and load vector, the above global matrices and global force vector can be respectively obtained:

$$\mathbf{K}^e = \begin{bmatrix} \mathbf{K}_{ww} & \mathbf{K}_{w\psi} \\ \mathbf{K}_{\psi w} & \mathbf{K}_{\psi\psi} \end{bmatrix}, \quad \mathbf{M}^e = \begin{bmatrix} \mathbf{M}_{ww} & \mathbf{M}_{w\psi} \\ \mathbf{M}_{\psi w} & \mathbf{M}_{\psi\psi} \end{bmatrix}, \quad \mathbf{F}^e = \begin{bmatrix} \mathbf{F}_w \\ \mathbf{F}_\psi \end{bmatrix} \quad (40)$$

where

$$\begin{aligned}
 \mathbf{K}_{ww} &= \int_0^l \left[(k_3 + k_4) \left(\frac{\partial^2 \mathbf{N}_w}{\partial x^2} \right)^T \frac{\partial^2 \mathbf{N}_w}{\partial x^2} + k_5 \left(\frac{\partial \mathbf{N}_w}{\partial x} \right)^T \frac{\partial \mathbf{N}_w}{\partial x} \right] dx \\
 \mathbf{K}_{w\psi} &= \int_0^l \left[(k_3 - 2k_4) \left(\frac{\partial^2 \mathbf{N}_w}{\partial x^2} \right)^T \frac{\partial \mathbf{N}_\psi}{\partial x} - k_5 \left(\frac{\partial \mathbf{N}_w}{\partial x} \right)^T \mathbf{N}_\psi \right] dx \\
 \mathbf{K}_{\psi w} &= \int_0^l \left[(k_3 - 2k_4) \left(\frac{\partial \mathbf{N}_\psi}{\partial x} \right)^T \frac{\partial^2 \mathbf{N}_w}{\partial x^2} - k_5 (\mathbf{N}_\psi)^T \frac{\partial \mathbf{N}_w}{\partial x} \right] dx \\
 \mathbf{K}_{\psi\psi} &= \int_0^l \left[k_1 \left(\frac{\partial^2 \mathbf{N}_\psi}{\partial x^2} \right)^T \frac{\partial^2 \mathbf{N}_\psi}{\partial x^2} + (k_2 + k_3 + 4k_4) \left(\frac{\partial \mathbf{N}_\psi}{\partial x} \right)^T \frac{\partial \mathbf{N}_\psi}{\partial x} + k_5 (\mathbf{N}_\psi)^T \mathbf{N}_\psi \right] dx
 \end{aligned} \tag{41}$$

$$\mathbf{F}_w = \int_0^l (\mathbf{N}_w)^T q(x) dx + \left[(\mathbf{N}_w)^T N_w^{(0)} + \left(\frac{\partial \mathbf{N}_w}{\partial x} \right)^T N_w^{(1)} \right] \Big|_0^L, \quad \mathbf{F}_\psi = 0 \tag{42}$$

$$\mathbf{M}_{ww} = \int_0^L m_0 (\mathbf{N}_w)^T \mathbf{N}_w dx, \quad \mathbf{M}_{\psi\psi} = \int_0^L m_2 (\mathbf{N}_\psi)^T \mathbf{N}_\psi dx, \quad \mathbf{M}_{w\psi} = \mathbf{M}_{\psi w} = 0 \tag{43}$$

From Eq. (41), it can be seen that there are three additional independent material length scale parameters in the stiffness matrix of the new Timoshenko beam element based on the strain gradient elasticity theory. This is different from classical Timoshenko beam theory, which just requires C_0 continuity. Thus the newly developed element makes it possible to capture the size effect. Verifications and numerical results are given in Section 4.

The boundary conditions for the Timoshenko beam based on the strain gradient theory can be written as

$$\left. \begin{aligned}
 \delta w = 0 \quad \text{or} \quad N_w^{(0)} = 0 \\
 \delta \delta w / \delta x = 0 \quad \text{or} \quad N_w^{(1)} = 0 \\
 \delta \psi = 0 \quad \text{or} \quad N_\psi^{(0)} = 0 \\
 \delta \delta \psi / \delta x = 0 \quad \text{or} \quad N_\psi^{(1)} = 0
 \end{aligned} \right\} x = 0, L \tag{44}$$

$N_w^{(0)}, N_w^{(1)}, N_\psi^{(0)},$ and $N_\psi^{(1)}$ are higher-order tractions; they have no special physical meaning and so are not considered here.

The kinematic boundary conditions in the newly proposed element are listed in Table 1. ‘‘S’’, ‘‘C’’, and ‘‘F’’ denote the boundary conditions of the edges as simply supported, clamped, and free, respectively. The dashes represent the unknown displacements at the corresponding boundary.

4. RESULTS AND DISCUSSION

In this section, the convergence of the present element is studied. Static bending and free vibration problems with a Timoshenko beam with simply supported and clamped boundary conditions are numerically solved by applying the new Timoshenko beam element. To verify the reliability and accuracy of the present approach, results obtained with

TABLE 1: Boundary conditions used in finite-element implementation

Boundary conditions	Node parameters related to bending deformation			
	w	w'	ψ	ψ'
S	0	—	—	0
C	0	—	0	—
F	—	—	—	—

the present element are compared with results from the literature (Wang et al., 2010). Unless otherwise indicated, the beam studied here is taken to be made of epoxy with the following properties (Lam et al., 2003; Wang et al., 2010): elastic modulus $E = 1.44$ GPa, density $\rho = 1,220$ kg/m³, Poisson’s ratio $\nu = 0.38$, material length scale parameter $l = 17.6$ μm , and shear coefficient $k_s = 5/6$.

4.1 Shear Locking Study

It is known that shear locking appears in the classical Timoshenko beam element when the length-to-thickness ratio is large. Here, the performance of the present Timoshenko beam element is illustrated when the thickness becomes very thin. For simplification, all three material length scale parameters are set to zero.

A simple beam subjected a concentrated force P at the midpoint is considered, as shown in Fig. 2. In Table 2, w_p and ψ_p are the deflection and rotation predicted by the present element when Poisson’s ratio is set to zero with different length-to-thickness ratios (L/h). The variables w_c and ψ_c are the deflection and rotation of the classical Euler-Bernoulli beam predicted by Eq. (45) with varying L/h (Gere, 2002).

$$w_c = \frac{PL^3}{48EI}; \quad \psi_c = \frac{PL^2}{16EI} \tag{45}$$

Table 2 shows that with an increase in L/h , the errors between the corresponding results predicted by the present element and those predicted by classical Euler-Bernoulli beam theory decrease; when L/h is very large, the errors can be ignored. This illustrates that the results obtained by the present element can reduce to the results of classical Euler-Bernoulli beam theory when the length-to-thickness ratio is very large and Poisson’s ratio is set to zero. Thus it can be guaranteed that the shear locking phenomenon does not exist here.

4.2 Convergence Study

As shown in Figs. 2 and 3, the static bending of a Timoshenko microbeam is solved to verify the convergence of the results. The dimensionless deflection and rotation results at point $x = L/4$ with simply supported and clamped boundary conditions are listed in Table 3. Equation (46) is adopted in the dimensionless treatment for convenience. From Table 3, it can be seen that the present element has good convergence and high precision. It can be also seen that

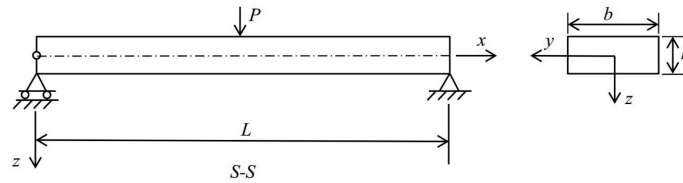


FIG. 2: Geometry and loading of the simply supported Timoshenko beam

TABLE 2: Deflection and rotation with different length-to-thickness ratios (L/h)

L/h	5	10	20	30	50	100
w_p	6.75563×10^{-8}	5.05023×10^{-7}	3.96933×10^{-6}	1.33522×10^{-5}	6.17107×10^{-5}	4.93331×10^{-4}
w_c	6.16517×10^{-8}	4.93213×10^{-7}	3.94571×10^{-6}	1.33168×10^{-5}	6.16517×10^{-5}	4.93213×10^{-4}
Error	9.577%	2.394%	0.599%	0.266%	0.096%	0.024%
ψ_p	2.23627×10^{-3}	8.54156×10^{-3}	3.37627×10^{-2}	7.57979×10^{-2}	2.10311×10^{-1}	8.40839×10^{-1}
ψ_c	2.10176×10^{-3}	8.40705×10^{-3}	3.36282×10^{-2}	7.56634×10^{-2}	2.10176×10^{-1}	8.40705×10^{-1}
Error	6.400%	1.600%	0.400%	0.178%	0.064%	0.016%

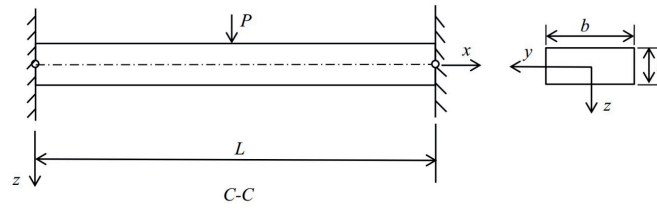


FIG. 3: Geometry and loading of the clamped Timoshenko beam

TABLE 3: Dimensionless deflection and rotation results at point $x = L/4$

Boundary conditions	Sources	Node parameters	Number of elements					
			4	8	12	16	20	100
S-S	a	\bar{w}	7.7369	7.7374	7.7375	7.7375	7.7375	7.7375
		$\bar{\psi}$	25.0810	25.0440	25.0407	25.0404	25.0403	25.0403
	b	\bar{w}	2.3390	2.3393	2.3393	2.3393	2.3393	2.3393
		$\bar{\psi}$	7.4715	7.4580	7.4579	7.4580	7.4580	7.4580
	c	\bar{w}	0.9170	0.9176	0.9176	0.9176	0.9176	0.9176
		$\bar{\psi}$	2.7257	2.7188	2.7185	2.7185	2.7185	2.7185
C-C	a	\bar{w}	1.4769	1.4773	1.4774	1.4774	1.4774	1.4774
		$\bar{\psi}$	8.3858	8.3504	8.3472	8.3468	8.3468	8.3468
	b	\bar{w}	0.5551	0.5840	0.5969	0.6030	0.6061	0.6100
		$\bar{\psi}$	2.6080	2.7279	2.7632	2.7793	2.7875	2.7981
	c	\bar{w}	0.2358	0.2364	0.2364	0.2364	0.2364	0.2364
		$\bar{\psi}$	0.9115	0.9042	0.9039	0.9039	0.9039	0.9039

Note: S-S: simply supported at both ends; C-C: clamped at both ends; a: classical theory; b: modified couple stress theory; c: present theory.

20 elements are enough to obtain reasonably accurate results. Unless otherwise indicated, 20 elements are used in all following computations.

For illustration purposes, the following parameters are used in computing the numerical results: $P = 100 \mu\text{N}$, $h = l$, $L = 20h$, and $b = 2h$.

$$\bar{w} = 1000w \frac{EJ}{PL^3}, \quad \bar{\psi} = 1000\psi \frac{EJ}{PL^2} \quad (46)$$

4.3 Verification Study

To verify the accuracy of the present element, some comparisons are given in Figs. 4–6. The value of the height of the Timoshenko microbeam is given in all figures. The three material length scale parameters (l_0 , l_1 , and l_2) are equal to the material length scale parameter l (i.e., $l_0 = l_1 = l_2 = l = 17.6 \mu\text{m}$). Other parameters are the same as those given earlier.

Figures 4 and 5 compare the static bending results of the simply supported Timoshenko microbeam predicted by the present element with results from the literature (Wang et al., 2010). It can be seen that the results obtained by the present model agree well with the theoretical results. When the element degenerates into the modified couple stress or classical Timoshenko beam element, the results also agree well (Wang et al., 2010). Figure 6 compares the natural frequencies of the simply supported Timoshenko microbeam predicted by the present element with those from the literature (Wang et al., 2010). The results predicted by the present model agree well with the theoretical results, meaning that this element has high reliability and accuracy.

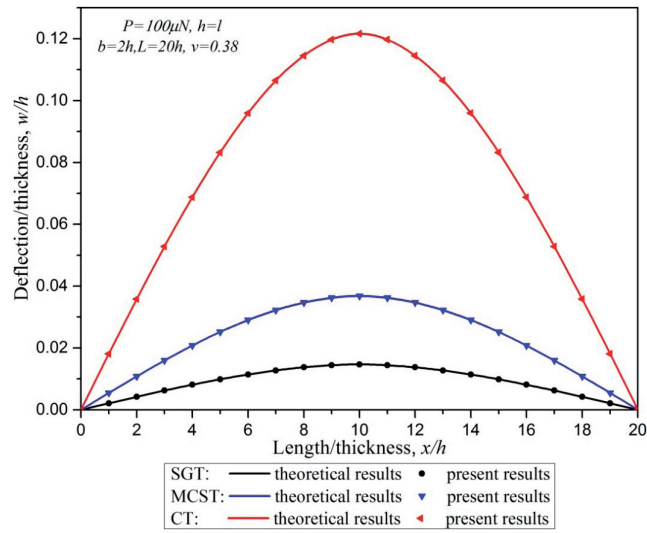


FIG. 4: Comparison of dimensionless deflection (w/h) from theoretical and present results

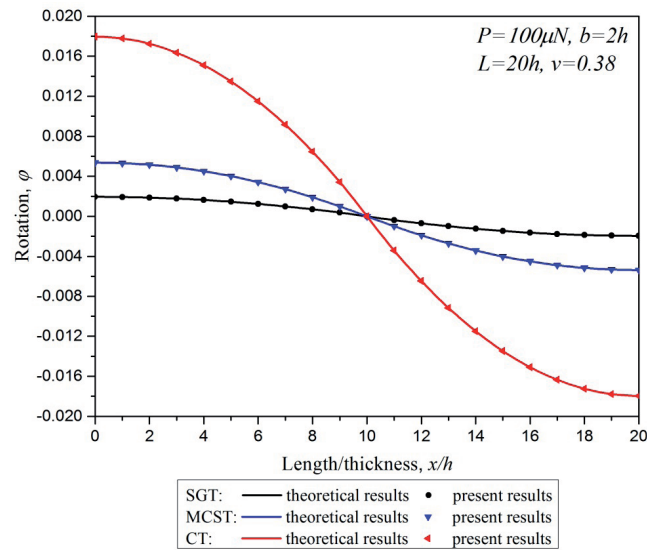


FIG. 5: Comparison of rotation from theoretical and present results

4.4 Static Bending of a Clamped Beam

Using the newly developed element, the static bending and free vibration problems of a clamped Timoshenko microbeam are investigated. The microbeam is subject to a concentrated force at the center point; the geometrical and load parameters are given in Figs. 7 and 8 and other parameters are the same as those given earlier. From Fig. 7, it can clearly be observed that the deflection predicted by the present element is smaller than that predicted by the classical element and the modified couple stress element. The absolute rotation values for the clamped Timoshenko microbeam predicted by the three models in Fig. 8 show a trend similar to that in Fig. 7. From both figures, it can be seen that there are large differences in deflection and rotation for the three models when the beam thickness h is equal

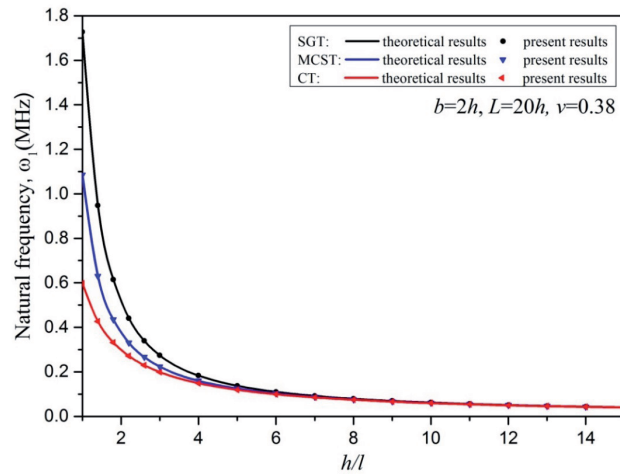


FIG. 6: Comparison of natural frequency from theoretical and present results

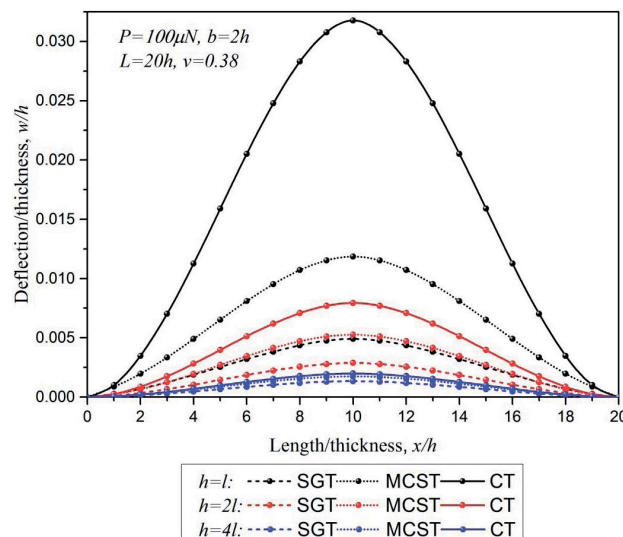


FIG. 7: Deflection of the clamped Timoshenko beam

to the material length scale parameter l . However, when the thickness of the beam becomes greater, such differences decrease. This shows that the size effect is significant only when the beam thickness is comparable to the material length scale parameter.

Figure 9 shows the change in the first-order natural frequency of the clamped Timoshenko beam predicted by the three models (the present model, the modified couple stress model, and the classical model) with the dimensionless thickness of the beam (h/l) for different values of Poisson's ratio ($\nu = 0$ and $\nu = 0.38$). It can be seen that the natural frequency predicted by the present element is not only larger than that predicted by the modified couple stress model but also larger than that predicted by the classical model for the two Poisson values. There are large differences in the natural frequency predicted by the three models for both cases, $\nu = 0$ and $\nu = 0.38$, when the dimensionless thickness of the beam is small ($h/l < 2$). When the thickness increases, the differences decrease or even disappear. This illustrates that the size effect is prominent when the beam thickness is as small as the material length scale parameter l . From

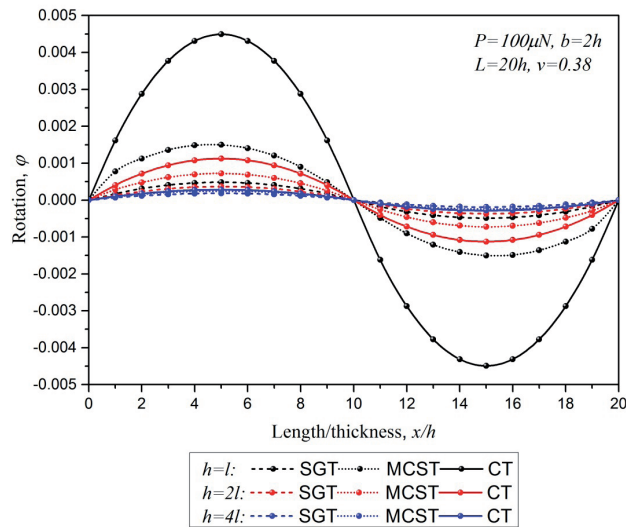


FIG. 8: Rotation of the clamped Timoshenko beam based on the three models with $h = l, 2l,$ and $4l$

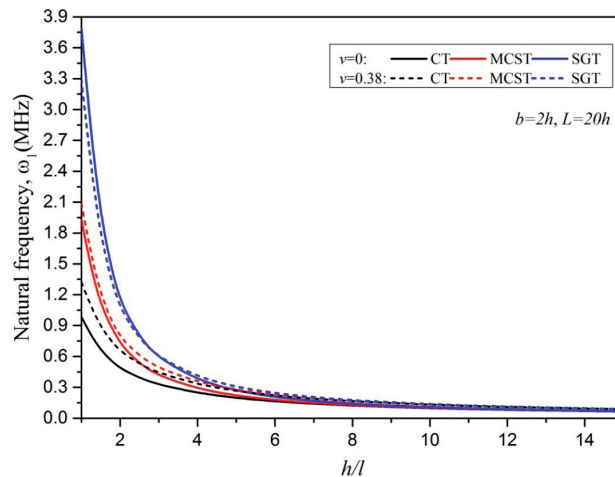


FIG. 9: Natural frequency of the clamped Timoshenko beam based on the three models with $\nu = 0$ and $\nu = 0.38$

Fig. 9, it can also be seen that the natural frequency with $\nu = 0.38$ is always larger than that with $\nu = 0$ for the classical model. However, this is not true for either the present model or the modified couple stress model.

5. CONCLUSIONS

A microscale Timoshenko beam element was developed based on the strain gradient elasticity theory. The proposed element contains three material length scale parameters that can capture the size effect. It is known that the classical Timoshenko beam element satisfies C_0 continuity, but the proposed element satisfies both C_0 continuity and C_1 weak continuity. Moreover, the new element can degenerate into the modified couple stress Timoshenko beam element or the classical Timoshenko beam element. The newly developed element comprises two nodes, with 4 DOF at each one considering only bending deformation.

Both the static bending and the free vibration problem of a simple beam are solved using the new element, and the results agree with those in the literature. Using this newly developed element, the static bending and free vibration problems of a clamped Timoshenko microbeam were investigated. Future work may focus on the plate and shell elements with strain gradient included.

ACKNOWLEDGMENTS

This work is supported by the National Natural Science Foundation of China (Grant Nos. 11202117 and 11272186), the Natural Science Fund of Shandong Province (BS2012ZZ006 and ZR2012AM014), and the Fundamental Research Funds of Shandong University (Grant No. 2015JX003).

REFERENCES

- Asghari, M., Ahmadian, M. T., Kahrobaian, M. H., and Rahaeifard, M., On the size-dependent behavior of functionally graded micro-beams, *Mater. Des.*, vol. **31**, no. 5, pp. 2324–2329, 2010a.
- Asghari, M., Kahrobaian, M. H., and Ahmadian, M. T., A nonlinear Timoshenko beam formulation based on the modified couple stress theory, *Int. J. Eng. Sci.*, vol. **48**, no. 12, pp. 1749–1761, 2010b.
- Asghari, M., Rahaeifard, M., Kahrobaian, M. H., and Ahmadian, M. T., The modified couple stress functionally graded Timoshenko beam formulation, *Mater. Des.*, vol. **32**, no. 3, pp. 1435–1443, 2011.
- Assadi, A., Size dependent forced vibration of nanoplates with consideration of surface effects, *Appl. Math. Model.*, vol. **37**, no. 5, pp. 3575–3588, 2013.
- Chasiotis, I. and Knauss, W. G., The mechanical strength of polysilicon films. II: Size effects associated with elliptical and circular perforations, *J. Mech. Phys. Solids*, vol. **51**, no. 8, pp. 1551–1572, 2003.
- Dym, C. L. and Shames, I. H., *Solid Mechanics: A Variational Approach*, New York: McGraw-Hill, 1973.
- Eringen, A. C., On differential-equations of nonlocal elasticity and solutions of screw dislocation and surface-waves, *J. Appl. Phys.*, vol. **54**, no. 9, pp. 4703–4710, 1983.
- Fathalilou, M., Sadeghi, M., and Rezazadeh, G., Micro-inertia effects on the dynamic characteristics of micro-beams considering the couple stress theory, *Mech. Res. Commun.*, vol. **60**, pp. 74–80, 2014.
- Gere, M. J., *Mechanics of Materials*, Beijing: China Machine Press, p. 632, 2002.
- Gurtin, M. E. and Murdoch, A. I., A continuum theory of elastic material surfaces, *Arch. Rat. Mech. Anal.*, vol. **57**, no. 4, pp. 291–323, 1975.
- Kahrobaian, M. H., Asghari, M., and Ahmadian, M. T., A Timoshenko beam element based on the modified couple stress theory, *Int. J. Mech. Sci.*, vol. **79**, pp. 75–83, 2014.
- Kahrobaian, M. H., Asghari, M., and Ahmadian, M. T., Strain gradient beam element, *Finite Elem. Anal. Des.*, vol. **68**, pp. 63–75, 2013.
- Koiter, W. T., Couple stress in the theory of elasticity I, II, *Proc. Kon. Nederl. Akad. Wetensch.*, vol. **B67**, pp. 17–44, 1964.
- Kong, S. L., Zhou, S. J., Nie, Z. F., and Wang, K., Static and dynamic analysis of micro beams based on strain gradient elasticity theory, *Int. J. Eng. Sci.*, vol. **47**, no. 4, pp. 487–498, 2009.
- Lam, D. C. C. and Chong, A. C. M., Indentation model and strain gradient plasticity law for glassy polymers, *J. Mater. Res.*, vol. **14**, no. 9, pp. 3784–3788, 1999.
- Lam, D. C. C., Yang, F., Chong, A. C. M., Wang, J., and Tong, P., Experiments and theory in strain gradient elasticity, *J. Mech. Phys. Solids*, vol. **51**, no. 8, pp. 1477–1508, 2003.
- Ma, H. M., Gao, X. L., and Reddy, J. N., A Microstructure-dependent Timoshenko beam model based on a modified couple stress theory, *J. Mech. Phys. Solids*, vol. **56**, no. 12, pp. 3379–3391, 2008.
- McFarland, A. W. and Colton, J. S., Role of material microstructure in plate stiffness with relevance to microcantilever sensors, *J. Micromech. Microeng.*, vol. **15**, no. 5, pp. 1060–1067, 2005.
- Mindlin, D., Micro-structure in linear elasticity, *Arch. Rational Mech. Anal.*, vol. **16**, no. 1, pp. 51–78, 1964.

- Park, S. K. and Gao, X. L., Bernoulli-Euler beam model based on a modified couple stress theory, *J. Micromech. Microeng.*, vol. **16**, pp. 2355–2359, 2006.
- Phadikar, J. K. and Pradhan, S. C., Variational formulation and finite element analysis for nonlocal elastic nanobeams and nanoplates, *Comput. Mater. Sci.*, vol. **49**, no. 3, pp. 492–499, 2010.
- Poole, W. J., Ashby, M. F., and Fleck, N. A., Micro-hardness of annealed and work-hardened copper polycrystals, *Scripta Materialia*, vol. **34**, no. 4, pp. 559–564, 1996.
- Pradhan, S. C., Nonlocal finite element analysis and small scale effects of CNTs with Timoshenko beam theory, *Finite Elem. Anal. Des.*, vol. **50**, no. 1, pp. 8–20, 2012.
- Sadeghian, H., Goosen, H., Bossche, A., Thijsse, B., and van Keulen, F., On the size-dependent elasticity of silicon nanocantilevers: Impact of defects, *J. Phys. D-Appl. Phys.*, vol. **44**, no. 7, 072001 (6 pp.), 2011.
- Tsiatas, G. C., A new Kirchhoff plate model based on a modified couple stress theory, *Int. J. Solids Struct.*, vol. **46**, no. 13, pp. 2757–2764, 2009.
- Vardoulakis, I., Exadaktylos, G., and Kourkoulis, S. K., Bending of marble with intrinsic length scales: A gradient theory with surface energy and size effects, *J. Phys. IV*, vol. **8**, no. P8, pp. 399–406, 1998.
- Wang, B., Zhao, J., and Zhou, S., A micro scale timoshenko beam model based on strain gradient elasticity theory, *Eur. J. Mech.–A/Solids*, vol. **29**, no. 4, pp. 591–599, 2010.
- Wang, B., Zhou, S., Zhao, J., and Chen, X., Pull-in instability analysis of electrostatically actuated microplate with rectangular shape, *Int J. Precis. Eng. Manuf.*, vol. **12**, no. 6, pp. 1085–1094, 2011a.
- Wang, B., Zhou, S., Zhao, J., and Chen, X., Size-dependent pull-in instability of electrostatically actuated microbeam-based MEMS, *J. Micromech. Microeng.*, vol. **21**, no. 2, 027001 (6 pp.), 2011b.
- Wang, B., Zhou, S., Zhao, J., and Chen, X., Pull-in instability of circular plate MEMS: A new model based on strain gradient elasticity theory, *Int. J. Appl. Mech.*, vol. **4**, no. 1, 1250003 (12 pp.), 2012.
- Wang, B., Liu, M., Zhao, J., and Zhou, S., A size-dependent Reddy–Levinson beam model based on a strain gradient elasticity theory, *Meccanica*, vol. **49**, no. 6, pp. 1427–1441, 2014.
- Xia, W., Wang, L., and Yin, L., Nonlinear non-classical microscale beams: Static bending, postbuckling and free vibration, *Int. J. Eng. Sci.*, vol. **48**, no. 12, pp. 2044–2053, 2010.
- Yang, F., Chong, A. C. M., Lam, D. C. C., and Tong, P., Couple stress based strain gradient theory for elasticity, *Int. J. Solids Struct.*, vol. **39**, no. 10, pp. 2731–2743, 2002.
- Yin, L., Qian, Q., and Wang, L., Size effect on the static behavior of electrostatically actuated microbeams, *Acta Mech. Sin.*, vol. **27**, no. 3, pp. 445–451, 2011.
- Zhang, B., He, Y., Liu, D., Gan, Z., and Shen, L., A non-classical mindlin plate finite element based on a modified couple stress theory, *Eur. J. Mech.–A/Solids*, vol. **42**, pp. 63–80, 2013.
- Zhang, B., He, Y. M., Liu, D. B., Gan, Z. P., and Shen, L., Non-classical timoshenko beam element based on the strain gradient elasticity theory, *Finite Elem. Anal. Des.*, vol. **79**, pp. 22–39, 2014.
- Zhao, J., Zhou, S., Wang, B., and Wang, X., Nonlinear microbeam model based on strain gradient theory, *Appl. Math. Model.*, vol. **36**, no. 6, pp. 2674–2686, 2012.

APPENDIX

The global stiffness matrix and the global mass matrix are expressed as follows:

$$\mathbf{K} = \begin{bmatrix} k_{11} & k_{12} & k_{13} & k_{14} & k_{15} & k_{16} & k_{17} & k_{18} \\ k_{21} & k_{22} & k_{23} & k_{24} & k_{25} & k_{26} & k_{27} & k_{28} \\ k_{31} & k_{32} & k_{33} & k_{34} & k_{35} & k_{36} & k_{37} & k_{38} \\ k_{41} & k_{42} & k_{43} & k_{44} & k_{45} & k_{46} & k_{47} & k_{48} \\ k_{51} & k_{52} & k_{53} & k_{54} & k_{55} & k_{56} & k_{57} & k_{58} \\ k_{61} & k_{62} & k_{63} & k_{64} & k_{65} & k_{66} & k_{67} & k_{68} \\ k_{71} & k_{72} & k_{73} & k_{74} & k_{75} & k_{76} & k_{77} & k_{78} \\ k_{81} & k_{82} & k_{83} & k_{84} & k_{85} & k_{86} & k_{87} & k_{88} \end{bmatrix}$$

$$\begin{aligned}
k_{11} = -k_{15} = -k_{51} = k_{55} &= \frac{12}{L^3}(k_3 + k_4) + \frac{6}{5L}k_5 \\
k_{13} = k_{17} = k_{31} = -k_{35} = -k_{53} = -k_{57} = k_{71} = -k_{75} &= \frac{6}{L^2}(k_3 + k_4) + \frac{1}{10}k_5 \\
k_{33} = k_{77} = \frac{4}{L}(k_3 + k_4) + \frac{2L}{15}k_5, \quad k_{37} = k_{73} = \frac{2}{L}(k_3 + k_4) - \frac{L}{30}k_5 \\
k_{12} = k_{16} = k_{21} = -k_{25} = -k_{52} = -k_{56} = k_{61} = -k_{65} &= \frac{1}{2}k_5 \\
k_{34} = k_{43} = -k_{78} = -k_{87} &= -\frac{1}{2}(k_3 - 2k_4) \\
k_{14} = -k_{18} = -k_{23} = k_{27} = -k_{32} = k_{36} = k_{41} = -k_{45} &= -\frac{1}{L}(k_3 - 2k_4) + \frac{L}{10}k_5 \\
-k_{54} = k_{58} = k_{63} = -k_{67} = k_{72} = -k_{76} = -k_{81} = k_{85} &= -\frac{1}{L}(k_3 - 2k_4) + \frac{L}{10}k_5 \\
-k_{38} = k_{47} = k_{74} = -k_{83} &= -\frac{1}{2}(k_3 - 2k_4) + \frac{L^2}{60}k_5 \\
k_{22} = k_{66} = \frac{12}{L^3}k_1 + \frac{6}{5L}(k_2 + k_3 + 4k_4) + \frac{13L}{35}k_5 \\
k_{24} = k_{42} = -k_{68} = -k_{86} = \frac{6}{L^2}k_1 + \frac{1}{10}(k_2 + k_3 + 4k_4) + \frac{11L^2}{210}k_5 \\
k_{26} = k_{62} = -\frac{12}{L^3}k_1 - \frac{6}{5L}(k_2 + k_3 + 4k_4) + \frac{9L}{70}k_5 \\
k_{28} = -k_{46} = -k_{64} = k_{82} = \frac{6}{L^2}k_1 + \frac{1}{10}(k_2 + k_3 + 4k_4) - \frac{13L^2}{420}k_5 \\
k_{44} = k_{88} = \frac{4}{L}k_1 + \frac{2L}{15}(k_2 + k_3 + 4k_4) + \frac{L^3}{105}k_5, \quad k_{48} = k_{84} = \frac{2}{L}k_1 - \frac{L}{30}(k_2 + k_3 + 4k_4) - \frac{L^3}{140}k_5
\end{aligned}$$

$$\mathbf{M} = \begin{bmatrix} m_{11} & m_{12} & m_{13} & m_{14} & m_{15} & m_{16} & m_{17} & m_{18} \\ m_{21} & m_{22} & m_{23} & m_{24} & m_{25} & m_{26} & m_{27} & m_{28} \\ m_{31} & m_{32} & m_{33} & m_{34} & m_{35} & m_{36} & m_{37} & m_{38} \\ m_{41} & m_{42} & m_{43} & m_{44} & m_{45} & m_{46} & m_{47} & m_{48} \\ m_{51} & m_{52} & m_{53} & m_{54} & m_{55} & m_{56} & m_{57} & m_{58} \\ m_{61} & m_{62} & m_{63} & m_{64} & m_{65} & m_{66} & m_{67} & m_{68} \\ m_{71} & m_{72} & m_{73} & m_{74} & m_{75} & m_{76} & m_{77} & m_{78} \\ m_{81} & m_{82} & m_{83} & m_{84} & m_{85} & m_{86} & m_{87} & m_{88} \end{bmatrix}$$

$$\begin{aligned}
mm_{11} = mm_{55} &= \frac{13}{35}m_0L, & mm_{13} = mm_{31} = -mm_{57} = -mm_{75} &= \frac{11}{210}m_0L^2 \\
mm_{15} = mm_{51} &= \frac{9}{70}m_0L, & -mm_{17} = mm_{35} = mm_{53} = -mm_{71} &= \frac{13}{420}m_0L^2 \\
mm_{33} = mm_{77} &= \frac{1}{105}m_0L^3, & mm_{37} = mm_{73} &= -\frac{1}{140}m_0L^3 \\
mm_{22} = mm_{66} &= \frac{13}{35}m_2L, & mm_{24} = mm_{42} = -mm_{68} = -mm_{86} &= \frac{11}{210}m_2L^2 \\
mm_{26} = mm_{62} &= \frac{9}{70}m_2L, & -mm_{28} = mm_{46} = mm_{64} = -mm_{82} &= \frac{13}{420}m_2L^2 \\
mm_{44} = mm_{88} &= \frac{1}{105}m_2L^3, & mm_{48} = mm_{84} &= -\frac{1}{140}m_2L^3
\end{aligned}$$